POLSKA AKADEMIA NAUK
INSTYTUT MASZYN PRZEPŁYWOWYCH

PRACE INSTYTUTU MASZYN PRZEPŁYWOWYCH

TRANSACTIONS OF THE INSTITUTE OF FLUID-FLOW MACHINERY

89

WARSZAWA – POZNAŃ 1989
PAŃSTWOWE WYDAWNICTWO NAUKOWE

PRACE INSTYTUTU MASZYN PRZEPŁYWOWYCH

poświęcone są publikacjom naukowym z zakresu teorii i badań doświadczalnych w dziedzinie mechaniki i termodynamiki przepływów, ze szczególnym uwzględnieniem problematyki maszyn przepływowych

*

THE TRANSACTIONS OF THE INSTITUTE OF FLUID-FLOW MACHINERY

exist for the publication of theoretical and experimental investigations of all aspects of the mechanics and thermodynamics of fluid-flow with special reference to fluid-flow machinery

---

REDAKCJA — EDITORIAL OFFICE

Instytut Maszyn Przepływowych PAN
ul. Gen. Józefa Fiszera 14, 80-952 Gdańsk, skr. pocztowa 621, tel. 41-12-71

Printed in Poland

ISBN 83-01-07072-2
ISSN 0079-3205

PAŃSTWOWE WYDAWNICTWO NAUKOWE - ODDZIAŁ W POZNANIU

Nakład 300+90 egz. Ark. wyd. 13,25. Ark. druk. 10,5. Papier offsetowy kl. IV, 71g.
B-1. Oddano do składania w kwietniu 1987 r. Podpisano do druku w marcu 1989 r.
Druk ukończono w grudniu 1989 r. Zam. 90/89 K-8/66
SKŁAD WYKONANO W ZAKŁADACH GRAFICZNYCH im. KEN W BYDGOSZCZY
DRUK ZAKŁAD POLIGRAFII WSP W ZIELONEJ GÓRZE

PRACE INSTYTUTU MASZYN PRZEPŁYWOWYCH
1989 Zeszyt 89

ANDRZEJ ZBOROWSKI, TRUONG SY KAP

Gdańsk

Investigation of the Ship Viscous Resistance Components and their Dependence on the Hull Form Parameters Based on the Body of Revolution Analogy

A method for calculating the ship friction resistance based on the Zazurca's proposal [1] was developed. The proposal deals mainly with a simple transformation of the actual ship form into a body of revolution for which characteristics of the potential flow and the boundary layer were calculated. Algorithms and computer programs were elaborated. Based on these programs systematic calculations were performed of the ship frictional resistance for about eighty ship forms for which results of model resistance tests were available. The ship forms used embrace a wide range of fullness. Calculations showed evidences of boundary layer separation, viz. for some forms of larger fullness the velocity of the potential flow and the shear stress reached the zero value at some distance from the trailing edge. The distance changed in a systematic way with the ship form parameters.

The method of friction resistance calculation was verified for a single case using experimental results for four geometrically similar models of the series 60 as published by Conn and Ferguson [3]. The comparison showed a satisfactory agreement between the calculated and measured values of the friction resistance components.

The calculated friction resistance of all the ship forms analysed was then compared with the viscous resistance of the forms obtained from the tank tests for the non-wave-making Froude number range. The excess of the viscous resistance over the friction resistance calculated was assumed to be the viscous pressure resistance. In this way the viscous resistance was split into the friction and pressure components. Both components found for all the models of the sample of forms collected were then analyzed by means of the regression analysis. The statistical generalization was proposed giving relation between the friction resistance, viscous pressure resistance, boundary layer separation length and the ship form parameter.

Nomenclature

B — breadth,
C_B — block coefficient,
C_F — friction resistance coefficient of the body,
C_{F0} — friction resistance coefficient of a flat plate,
C_P — viscous pressure coefficient,
C_S — separation drag coefficient,
C_V — viscous resistance coefficient,
F_n — Froude number,
H — shape factor $\left(\frac{\delta^*}{\theta}\right)$,
H_S — shape factor at the point of flow separation,
k_1, k_2 — form factors,
L — length,
R_n — Reynolds number,
X_B — longitudinal position of the centre of buoyancy,
X_S — relative length of the separation area $\left(\frac{X_S}{L}\right)$,

S_S — section area at the point of the flow separation,
S_M — midship section area,
$\overline{S}_S = S_S/S_M$,
δ — boundary layer thickness,
δ^* — boundary layer displacement thickness,
θ — boundary layer momentum thickness,

1. Introduction

In view of lack of any consistent theory for calculation of the ship friction and viscous resistance simplified theoretical and experimental models have been adopted since W. Froude famous plank work. His conception of the equivalent flat plate has been used up to date with only a few additional assumptions. A more recent approach is that of using a body of revolution as a model of ship form; this enables resistance and propulsion characteristics of a ship to be assumed on a more rational basis [4, 5, 6].

The possibility of modelling the ship hydrodynamic characteristics by means of those of a body of revolution has been examined over the last decade by different authors. To mention some of them, the work done by Matheson, Joubert and others from the University of Melbourne should be pointed out. These authors examined in a series of papers the use of a body of revolution as a model of reflex ship forms for the estimation of skin friction. In their last paper, after a careful and comprehensive experimental and theoretical study, they came to the conclusion that a body of revolution based on the equality of perimeter variation is not a good hydrodynamic model of a reflex ship hull form [7].

Similar approach was taken by Zazurca [1]. He used the pressure field calculated for an equivalent body of revolution to estimate the ship skin friction resistance. This approach, despite of its inadequacy as mentioned above, was adopted in the present work to perform systematic calculation of the ship friction resistance for different hull forms and to investigate how the viscous resistance components are changing with form parameters. Appendices 1 and 2 give some details of the calculation methods adopted. Respective algorithms and description of the computer programs are given in [2].

The results of exemplary calculations of velocity potential, velocity distribution over the length of the hull, boundary layer characteristics and viscous resistance components for a tanker model are given in Appendix 3.

The suggested calculation method was verified using some experimental results. Such a verification is usually limited by lack of experimental data on skin friction of ship forms. Direct measurements of skin friction are scarcely available and often not reliable as the measurement techniques have not been developed sufficiently well. For the purpose of the present analysis the friction resistance of our geosim models of the series 60 found indirectly from the measurements of pressure distribution as performed by Conn and Ferguson [3] was used. From the experiment the pressure resistance of the models was estimated and deducted from the total resistance, giving the model frictional resistance. The experiment was carried out in the range of Reynolds numbers from 9.5×10^5 to 3.9×10^6. In Fig. 1 the friction resistance

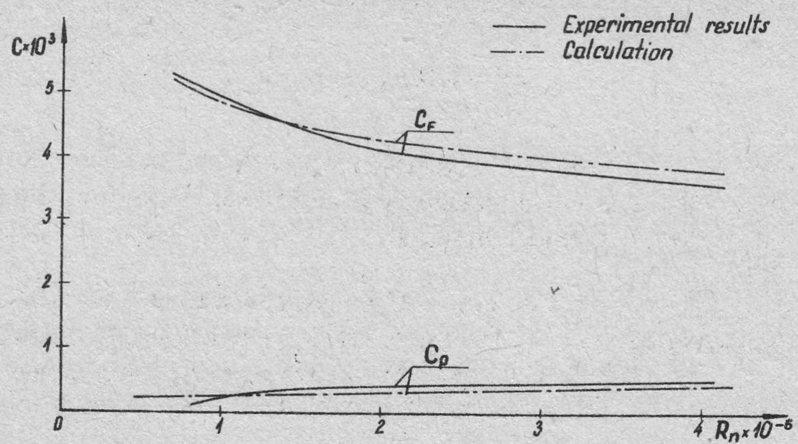

Fig. 1. Comparison between experimental and calculated friction and pressure resistance coefficients

Table 1
Results of calculation of friction and pressure resistance coefficients for 60-series models, $C_B = 0.60$, speed-length ratio 0.56

$R_n\ 10^{-6}$	0.948	1.539	2.309	3.889
$C_F\ 10^3$	4.954	4.418	4.035	3.617
$C_P\ 10^3$	0.210	0.421	0.429	0.531

coefficient C_F estimated experimentally is given for the speed-length ratio equal to 0.56 (Froude number 0.166). The values of frictional resistance coefficient calculated by means of the theoretical method adopted are given in Table 1 for four geometrically similar models investigated by Conn and Fergúson. Fig. 1 shows comparison between the friction resistance coefficients calculated and found experimentally. The comparison shows good agreement between the experiment and the theory adopted for the case considered.

2. Evaluation of viscous resistance components

The described method for calculating the skin friction resistance of a ship form was used to split the viscous resistance measured on ship models in the non-wave-making Froude number range into two main components, viz. the friction and pressure resistance. This can be expressed in terms of nondimensional coefficients as follows:

$$C_V = C_F + C_P. \tag{1}$$

Both the resistance components are assumed to be dependent on the body form and the Reynolds number.

To find the necessary Reynolds number function it can be assumed further on that both resistance components are proportional to the flat plate friction resistance C_{FO}

$$C_F = (1+k_1)C_{FO}, \tag{2}$$
$$C_P = k_2 C_{FO}, \tag{3}$$

where k_1 and k_2 the are so called form factors which express the influence of the form characteristics on the skin friction and pressure resistance, respectively. Equations (2) and (3) can be accepted only under assumption that both k_1 and k_2 are not functions of the Reynolds number.

The conception of form factors k_1 and k_2 is convenient in some ship resistance analyses due to the fact that the complex viscous resistance function can simply be represented as a product of two functions, viz. a function of the form parameters (k_1 and k_2) and a function C_{FO} of the Reynolds number. Substituting (2) and (3) into (1) we have

$$C_V = (1+k_1)C_{FO} + k_2 C_{FO} \tag{4}$$

or

$$C_V = (1+k_1+k_2)C_{FO}. \tag{5}$$

Knowing the form factors $(1+k_1)$ and k_2 it is possible to estimate the friction and pressure resistance and the viscous resistance of the ship form.

In the present paper both viscous resistance components are analyzed in terms of the form factors $(1+k_1)$ and k_2. The way by which the form factors are estimated is a combination of theoretical and statistical approaches embracing the following steps:

a) with the aid of the equivalent body of revolution method as described in Appendices 1 and 2 the skin friction resistance for 86 models of available ship forms is calculated. Hence the value of C_F in equation (1) can be found.

b) From equation (2) the form factor $(1+k_1)$ is deduced as

$$1+k_1 = \frac{C_F}{C_{FO}}, \tag{6}$$

where C_{FO} is the ITTC-1957 friction resistance coefficient for a flat plate,

$$C_{FO} = \frac{0.075}{(\log R_n - 2)^2}. \tag{7}$$

c) The viscous resistance coefficient C_V in eq. (1) is found from known model test results of the ship forms considered for the non-wave-making Froude number range.

d) The viscous pressure resistance in the present analysis is defined as the difference between the viscous resistance measured and the calculated friction resistance

$$C_P = C_V - C_F. \tag{8}$$

The viscous pressure resistance coefficient C_P estimated in this way for four geometrically similar models of the series 60 is compared in Fig. 1 with the pressure resistance found experimentally by Conn and Ferguson [3].

e) The form factor k_2 is estimated from eq. (3) as

$$k_2 = \frac{C_P}{C_{FO}}. \tag{9}$$

The proposed method of analysis has been verified preliminarily by systematic calculation of the resistance components and the range of separation for ship forms of different fullness and Reynolds numbers. By assessment of the trends of variation of these characteristics with form parameters and Reynolds number the method can be evaluated. Table 2 shows the results of calculations of the Reynolds number influence

Table 2

Influence of the Reynolds number on the resistance components, $C_B =$ $= 0.65$, $F_n = 0.17$

$10^6 R_n$	0.9484	1.5387	2.3087	3.8895
$10^3 C_{FO}$	4.742	4.277	3.939	3.560
$10^3 C_T$	5.165	4.842	4.464	4.148
$10^3 C_F$	4.902	4.536	4.206	3.792
$10^3 C_P$	0.263	0.306	0.355	0.356
$1+k_1$	1.034	1.061	1.065	1.065
k_2	0.055	0.072	0.090	0.200

on the resistance components and the form factors for four geosim" models of the series 60 ($C_B = 0.65$). It can be seen from the table that the variation of the factors with the Reynolds number is negligibly small except for the smallest model ($R_n =$ $= 0.95 \times 10^6$), for which the discrepancy obtained can be explained by the inadequacy of the ITTC basic line used for the region of small R_n.

Table 3

Influence of the Reynolds number and block coefficient on the length of separation $\overline{X}_S$

C_B \ R_n	7.768×10^5	1.260×10^6	1.891×10^6	3.271×10^6	5.894×10^6	9.563×10^6	4.636×10^7	2.335×10^8	7.311×10^8	1.125×10^9
0.65	—	—	—	—	—	—	—	—	—	—
0.70	0.630	0.573	0.544	0.513	0.503	0.493	0.480	0.480	0.480	0.480
0.75	2.414	2.305	2.252	2.240	2.190	2.186	2.172	2.172	2.172	2.172
0.80	2.895	2.805	2.715	2.678	2.668	2.657	2.667	2.667	2.647	2.647

Table 3 presents the results of calculation of the relative length of separation $\overline{X}_S$ zone as defined in Appendix 3. The calculations were performed for four series of geosim" models of different block coefficients. In this way the influence of the fullness and Reynolds number could be studied. It can be seen from the table that the suggested method gives the results which could be expected in advance, viz. that with an increase of fullness the range of separation increases. No separation was found for the block coefficient 0.65. Also the increase of the Reynolds number leads to reduction of the separation region unless the Reynolds number is greater than 10^7.

The calculation shows that beyond this value the range of separation does not vary with the Reynolds number.

3. Discussion of the assumptions made

The basic assumption of the suggested method as used in the present analysis, viz. that the form function $k = 1+k_1+k_2$ (eq. (5)) is independent of the Reynolds number, requires more detailed discussion in the light of the results of recent investigations of the problem.

The research work carried out by Gadd on doubled models in the wind tunnel [8] showed that the above assumption is not satisfied only in the case of large separation area on the body surface. If no separation occurs or its region is restricted to a rather small area and the line of separation shifts towards the end of the body with increasing Reynolds number then it can be assumed that k is only a function of form characteristics of the body and does not depend on the Reynolds number. In practice this assumption is fulfilled for large models of even full forms ($C_B = 0.83$) provided that R_n is greater than $4 \cdot 10^6$. According to results obtained by Gadd it can be further assumed for such forms that the viscous resistance C_V (embracing the friction and pressure resistances) is proportional to the skin friction resistance of the plank as expressed by eq. (5). It was also shown that the hypothesis of proportionality is not satisfied in the case of bodies with large separation area or bodies with fixed separation point as, for instance, ship models with transom stern. For such forms separation drag does not change with the Reynolds number. However, because the friction resistance decreases with increasing R_n the proportion of the separation drag in the viscous resistance increases. Therefore it can not be assumed in this case that the viscous resistance is proportional to the skin friction of a plank. The separation drag or base drag of forms with transom stern is relatively higher for the normal size than on a model.

For the forms of large separation area or forms with transom stern having constant separation drag with variation of R_n the following relation has been suggested [9] in place of equation (5)

$$C_V = (1+k_1)C_{F0}+C_S, \tag{10}$$

where C_S is the separation drag coefficient (or the base drag coefficient).

From the point of view of scaling laws of the ship resistance all hull forms can be divided into streamlined bodies if they follow equation (5) and bluff bodies if their drag coefficients satisfy equation (10). The resistance components C_P in eq. (1) and C_S in eq. (10) are due to the pressure difference and both are components of viscous pressure resistance. They follow different scaling laws and therefore should be considered separately.

The object of the next part of the work is to examine the effect of the form parameters variations on the viscous resistance components defined by equations (4) or (5). This is done by analyzing the form factors k_1 and k_2 as dependent only on the ship form.

4. Influence of form parameters on the viscous resistance components and length of separation area

The problem how the form parameters affect the viscous resistance components and separation area has been studied by means of a statistical method. First of all 86 statistical data were collected in connection with model test results of ship forms having block coefficients between 0.50 and 0.90. The data were taken from [9, 10, 11 and 12].

For these models the friction resistance coefficient C_F, pressure resistance coefficient C_P, separation area $\overline{X}_S$ and form factors $(1+k_1)$ and k_2 were calculated by means of the method described in section 2. The results of calculation are given in Table 4 for $C_B > 0.8$, and in Table 5 for $C_B \leqslant 0.8$, together with geometrical particularities of the models. These values were plotted to find how the considered hydrodynamic characteristics correlate with the form parameters. Examples of the plots

Table 4

Form parameters and hydrodynamic characteristics calculated for the ship model, $C_B > 0.8$

No.	$C_{F0} \times 10^3$	B/T	L/B	L/T	C_B	$\overline{X}_{CB}$	$\overline{\omega}_S$	$\overline{X}_s$	$C_V \times 10^3$	$C_V \times 10^3$	$1+k_1$	k_2
1	5,817	2,063	5,934	27,670	0,834	−3,993	0,514	3,90	4,1046	3,8684	1,310	0,080
2	5,504	2,760	7,042	19,351	0,831	3,20	0,520	5,00	4,3258	4,0663	1,377	0,089
3	5,063	3,120	5,917	18,484	0,849	−2,0	0,424	4,25	4,1401	3,8684	1,31	0,092
4	6,579	2,630	9,709	25,510	0,583	1,8	0,560	4,50	4,0072	3,7267	1,262	0,095
5	6,682	2,750	9,434	27,933	0,862	1,6	0,480	5,25	4,0545	3,7208	1,260	0,113
6	6,752	3,950	9,615	28,409	0,884	1,2	0,711	6,25	4,0869	3,7326	1,264	0,120
7	6,398	2,500	9,150	24,213	0,896	1,1	0,800	7,25	4,1283	3,7503	1,270	0,128
8	5,446	2,710	6,993	19,011	0,821	4,2	0,266	4,25	4,3011	4,0413	1,369	0,088
9	5,458	2,620	7,143	18,657	0,821	3,1	0,324	4,38	4,1578	3,9541	1,339	0,069
10	5,774	2,600	7,813	20,243	0,825	2,9	0,219	3,63	4,1578	3,9393	1,334	0,074
11	5,385	2,620	7,042	18,450	0,829	5,1	0,289	4,38	4,2346	3,9925	1,352	0,082
12	5,385	2,320	7,042	18,450	0,815	5,1	0,289	4,38	4,1638	3,9482	1,337	0,073
13	5,417	2,620	7,042	18,450	0,830	4,6	0,316	4,00	4,0869	3,7857	1,282	0,102
14	5,156	2,120	7,299	15,432	0,824	3,3	0,327	4,00	4,1342	3,9216	1,328	0,072
15	5,350	3,200	6,350	22,727	0,825	3,3	0,290	2,75	4,0309	3,8094	1,290	0,075
16	4,062	2,100	6,325	15,733	0,814	−0,1	0,240	1,88	4,2228	4,0456	1,370	0,060
17	5,801	2,600	7,875	20,284	0,815	2,8	0,050	1,88	3,8832	3,6765	1,245	0,070
18	5,575	2,760	7,143	19,724	0,819	3,6	0,333	3,4	4,3202	4,0544	2,373	0,090
19	5,805	4,30	7,813	20,336	0,870	2,50	0,300	4,75	3,9983	3,6676	1,242	0,112
20	5,805	2,60	9,153	20,336	0,819	3,10	0,300	3,25	4,0456	3,8448	1,302	0,068
21	5,646	2,50	7,634	19,047	0,801	2,40	0,386	2,75	4,0013	3,8094	1,240	0,065
22	5,521	2,69	7,092	19,120	0,801	3,20	0,040	1,25	3,9895	3,8300	1,297	0,054
23	5,509	2,71	6,992	19,011	0,802	4,20	0,060	1,50	4,0456	3,8802	1,314	0,056
24	4,954	4,14	8,787	20,450	0,804	1,10	0,280	3,38	3,8923	3,7119	1,257	0,061
25	5,373	2,30	6,711	18,656	0,805	3,10	0,355	3,38	4,2021	4,0102	1,358	0,065
26	5,610	3,68	7,576	18,868	0,807	3,00	0,157	1,63	3,9718	3,7769	1,279	0,066
27	5,610	3,00	7,519	18,797	0,793	3,85	0,090	1,63	3,9688	3,8182	1,293	0,051
28	5,375	4,06	8,400	18,182	0,853	1,91	0,384	4,38	3,9806	3,6410	1,233	0,115
29	5,495	4,66	8,525	18,182	0,798	2,04	0,060	1,50	3,7089	3,5554	1,204	0,052
30	5,483	3,40	7,273	18,182	0,840	0,95	0,297	3,62	4,0660	3,8153	1,292	0,085
31	5,464	3,50	7,273	18,182	0,802	2,00	0,308	4,25	3,9482	3,7474	1,269	0,068
32	5,477	3,32	8,273	18,182	0,845	4,90	0,296	3,75	5,0663	3,7710	1,277	0,100
33	5,434	2,50	7,273	18,182	0,826	1,96	0,707	5,00	3,9777	3,6913	1,250	0,097
34	5,260	2,65	6,631	17,543	0,810	4,50	0,150	2,25	4,1312	3,9688	1,344	0,055
35	5,477	2,50	6,750	18,182	0,802	2,08	0,329	2,50	4,0220	3,8448	1,302	0,060
36	4,918	2,82	6,650	18,083	0,800	1,50	0,212	2,75	3,9540	3,7857	1,282	0,057

Form parameters and hydrodynamic characteristics calculated for the ship model, $C_B < 0.8$

No.	Model	C_B	L/B	B/T	$\overline{\omega}_s = \frac{\omega_s}{\omega_m}$	$\overline{X}_s$ $(T=T)$	$\overline{X}_s$ $(T=0.75\,T)$	$\overline{X}_s$ $(T=0.5\,T)$	$\overline{X}_s$ $(T=0.25\,T)$	$C_T \cdot 10^3$	$C_F \cdot 10^3$	$C_P \cdot 10^3$	$1+k_1 = C_F/C_{F_0}$	$k_2 = \frac{C_P}{C_{P_0}}$	H_s	$C_{F_0} \cdot 10^3$ Wg ITTC 57
1	4210-W	0,60	7,5	2,5	—	—	—	—	—	3,8837	3,8355	0,0482	1,194	0,015	—	3,211
2	4252	0,60	6,5	3,0	—	—	—	—	—	4,0050	3,8766	0,1284	1,207	0,040	—	3,211
3	4255	0,60	7,5	3,0	—	—	—	—	—	3,8810	3,7782	0,1028	1,177	0,032	—	3,211
4	4254	0,60	8,5	3,0	—	—	—	—	—	3,8720	3,8238	0,0482	1,191	0,015	—	3,211
5	4241	0,60	7,5	3,5	—	—	—	—	—	4,0330	3,8275	0,2055	1,191	0,064	—	3,211
6	4253	0,60	7,5	3,5	—	—	—	—	—	3,909	3,8416	0,0674	1,197	0,021	—	3,211
7	4242	0,60	8,5	3,5	—	—	—	—	—	3,911	3,8468	0,0642	1,196	0,020	—	3,211
8	4211-W	0,65	7,25	2,50	—	—	—	—	—	3,9458	3,8816	0,0642	1,208	0,020	—	3,211
9	4272	0,65	6,25	3,00	—	—	—	—	—	3,993	3,8142	0,1798	1,190	0,056	—	3,211
10	4275	0,65	7,25	3,00	—	—	—	—	—	4,002	3,8222	0,1798	1,190	0,056	—	3,211
11	4274	0,65	8,25	3,00	—	—	—	—	—	3,892	3,8246	0,0674	1,191	0,021	—	3,211
12	4265	0,65	6,25	3,50	—	—	—	—	—	4,025	3,8195	0,2055	1,189	0,064	—	3,211
13	4273	0,65	7,25	3,50	—	—	—	—	—	3,918	3,7799	0,1381	1,177	0,043	—	3,211
14	4266	0,65	8,25	2,50	—	—	—	—	—	3,890	3,829	0,0610	1,192	0,019	—	3,211
15	4212-W	0,70	7,00	2,50	—	0,533	—	—	—	3,9438	3,7511	0,1927	1,168	0,060	2,480	3,211
16	4256	0,70	6,00	3,00	—	1,098	—	—	—	4,139	3,8243	0,3147	1,191	0,098	2,140	3,211
17	4259	0,70	7,0	3,00	—	—	—	—	—	4,047	3,8351	0,2119	1,142	0,066	—	3,211
18	4258	0,70	8,00	3,00	—	—	—	—	—	3,891	3,7754	0,1156	1,176	0,036	—	3,211
19	4245	0,70	6,00	3,50	—	0,545	—	—	—	4,032	3,7912	0,2408	1,181	0,075	2,338	3,211
20	4257	0,70	7,00	3,50	—	—	—	—	—	4,058	3,8076	0,2504	1,186	0,078	—	3,211
21	4246	0,70	8,00	3,50	—	—	—	—	—	3,979	3,7863	0,1927	1,179	0,060	—	3,211
22	4213-W	0,75	6.75	2,50	—	1,9314	2,6534	—	—	4,0971	3,8531	0,2440	1,200	0,076	2,50	3,211
23	4276	0,75	5,75	3,00	—	2,079	2,929	—	—	4,195	3,8546	0,3404	1,204	0,106	2,709	3,211
24	4279	0,75	6,75	3,00	—	1,557	2,402	—	—	3,982	3,7926	0,1894	1,181	0,059	2,500	3,211
25	4278	0,75	7,75	3,00	—	1,058	—	—	—	3,929	3,8006	0,1284	1,183	0,040	2,30	3,211
26	4269	0,75	5,75	3,50	—	1,868	2,696	—	—	4,122	3,8555	0,2665	1,201	0,828	2,40	3,211
27	4277	0,75	6,75	3,50	—	1,271	2,066	—	—	3,9701	3,7871	0,1830	1,179	0,057	2,20	3,211
28	4214-W	0,80	6,50	2,5	—	2,795	4,276	—	—	4,1905	3,8565	0.2344	1,230	0,073	2,446	3,211
29	4260	0,80	5,50	3,0	—	3,025	4,047	—	—	4,434	4,0904	0,3436	1,274	0,107	2,50	3,211
30	4263	0,80	6,50	3,0	—	3,048	4,322	3,404	—	4,102	3,8034	0,2986	1,185	0,093	2,20	3,211
31	4262	0,80	7,50	3,0	—	2,95	3,825	2,640	—	3,999	3,8013	0,1927	1,184	0,060	2,20	3,211
32	4249	0,80	5,5	3,5	—	3,438	4,152	3,648	—	4,262	3,9698	0,2922	1,237	0,091	2,626	3,211
33	4261	0,80	6,5	3,5	—	2,998	4,019	2,882	—	4,064	3,820	0,2440	1,189	0,076	2,501	3,211
34	4250	0,80	7,5	3,5	—	2,792	3,644	3,214	—	4,005	3,7834	0,2216	1,078	0,069	2,525	3,211
35	835	0,585	7,235	2,40	—	—	—	—	—	3,7360	3,6862	0,0498	1,184	0,016	—	3,114
36	833	0,610	7,235	2,40	—	—	—	—	—	3.7449	3,6826	0,0623	1,183	0,020	—	3,114
37	795	0,634	7.235	2,40	—	—	—	—	—	3,6949	3,6233	0,0716	1,164	0,023	—	3,114

38	720	0,658	7,235	2,40	—	—	—	—	—	3,7645	3,6711	0,0934	1,179	0,030	—	3,114
39	796	0,683	7,235	2,40	—	0,906	—	—	—	3,8609	3,6678	0,1931	1,178	0,062	2,11	3,114
40	719	0,707	7,235	2,40	—	1,061	—	—	—	3,8826	3,6646	0,2180	1,177	0,070	2,34	3,114
41	834	0,732	7,235	2,4	—	1,628	—	—	—	3,8959	3,6623	0,2336	1,178	0,075	2,635	3,114
42	251-A1	0,518	7,070	2,25	—	—	—	—	—	5,220	5,1666	0,0534	1,160	0,012	—	4,453
43	251-A2	0,518	7,97	3,25	—	—	—	—	—	5,250	5,1565	0,0935	1,158	0,021	—	4,453
44	249-A3	0,518	8,916	2,25	—	—	—	—	—	5,170	4,6802	0,4898	1,153	0,100	—	4,453
45	269-R0	0,518	6,775	3,35	—	—	—	—	—	5,215	5,1215	0,0935	1,160	0,021	—	4,453
46	264-R1	0,605	7,013	3,35	—	1,168	—	—	—	5,280	5,117	0,1603	1,150	0,036	2,196	4,453
47	267-R2	0,645	7,25	3,35	—	2,126	—	—	—	5,455	5,2324	1,2226	1,174	0,050	2,384	4,453
48	260-D2	0,518	5,65	3,90	—	—	—	—	—	5,360	5,1772	0,1826	1,162	0,041	—	4,453
49	261-E2	0,523	5,65	4,45	—	—	—	—	—	5,525	5,3914	0,1336	1,22	0,030	—	4,453
50	270-R2	0,60	7,67	2,80	—	1,174	—	—	—	5,320	5,1330	0,1870	1,15	0,042	2,319	4,453

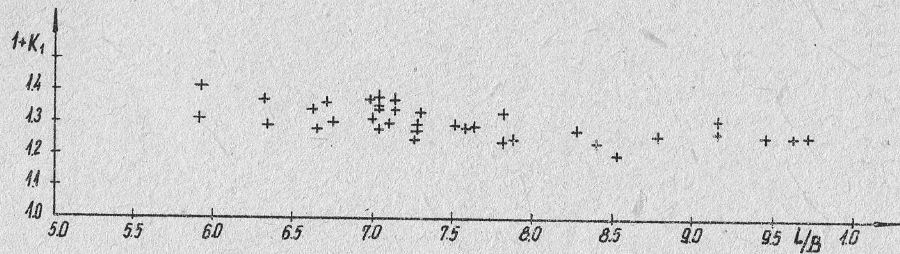

Fig. 2. Relation between form factor $(1+k_1)$ and L/B for $C_B > 0.8$

Fig. 3. Relation between separation area $\overline{X}_S$ and L/B for $C_B > 0.8$

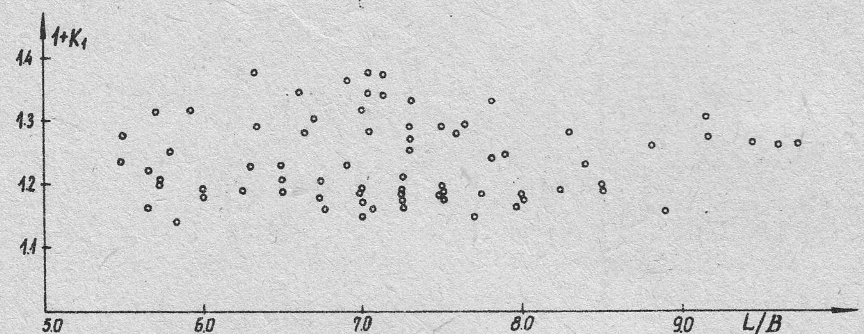

Fig. 4. Relation between form factor $(1+k_1)$ and L/B for $C_B > 0.8$

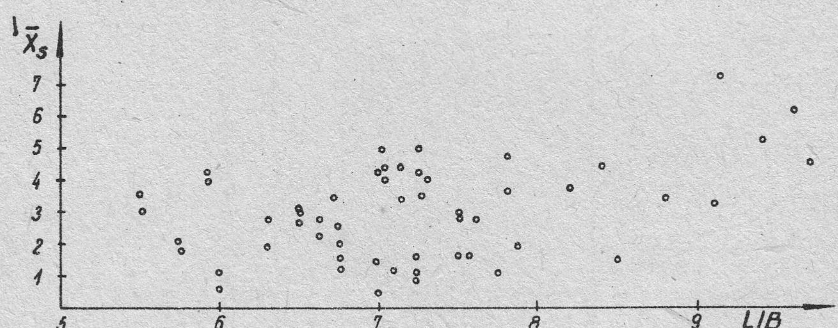

Fig. 5. Relation between separation area $\overline{X}_S$ and L/B for $C_B > 0.8$

are shown in Figs. 2 to 5*. The plots show a distinct trend of changing the form factors $(1+k_1)$ and k_2 and separation area $\overline{X}_S$ with the length-breadth ratio L/B, breadth-draught ratio B/T, block coefficient C_B and longitudinal position of the centre of buoyancy X_B. Also the relation between the form factor k_2 and the relative transverse section area at which separation of flow occurs $\overline{S}_S$ was established (with $\overline{S}_S = S_S/S_M$, S_M being the midship section area and the subscript S designating the point of separation).

In Table 5 there are included the values of separation area X_S calculated for

* For the complete set of plots see: Truong Sy Kap, D. Sc. Thesis, Technical University of Gdańsk

different draughts T, 0.75 T, 0.5 T, and 0.25 T. Table 5 includes also the shape factor H_s which is the ratio of the displacement thickness of the boundary layer δ^* and momentum thickness θ calculated for the point of separation of the models with separated flow. It can be pointed out that separation in two-dimensional turbulent boundary layer occurs at $H_s = 1.8 - 2.4$. Extension of the two-dimensional boundary layer theory to the special three-dimensional case of a plane of symmetry, made by Johnson, yielded the criterion of separation $H_s = 1.8$ [14]. As it is seen from Table 5 the shape factor H_s for all the models with separated flow is larger than 2.

The relations between the hydrodynamic characteristics considered and the form parameters were found by statistical method based on the regression analysis and the least square method. When forming the equations, conclusions drawn from correlation plots were taken into account as far as the trend of a particular relationship was concerned. The details of the statistical approach are given in [15]. In that reference different equations were tried and solved by statistical method using the data from Tables 4 and 5. Some combinations of form parameters tried were complex and led to complicated relationships. They enabled the study of influence of form parameters to be performed as did the data included in Tables 4 and 5. Some efforts were also undertaken to obtain certain simplified formulations for calculation $(1+k_1)$, k_2 and $\bar{X}_S$. These are as follows

$$1+k_1 = 1.15 + 14.636 \frac{C_B^2}{\left(\frac{L}{B}\right)^2 \cdot \frac{B}{T}}, \tag{11}$$

$$\bar{X}_S = 12.137 \frac{C_B \bar{S}_S^{1/2}}{\left(\frac{L}{B}\right)^{1/2}} + 1.279, \tag{12}$$

$$k_2 = 0.0177 + 0.5731 \frac{C_B^2}{\left(\frac{L}{B}\right)^{1/2} \cdot \frac{B}{T}} \quad \text{for } C_B < 0.8, \tag{13}$$

$$k_2 = 0.048 \frac{C_B^2 \bar{X}_S}{\left(\frac{L}{B}\right)^{1/2}} + 0.02 \quad \text{for } C_B > 0.8.$$

5. Conclusions

To study the complex three-dimensional flow around the ship form an analogy with a body of revolution was applied. The simulation of the real ship flow by that of the simplified form, although inadequate from theoretical point of view, leads to some conclusions which can have practical significance, particularly when the results obtained are treated in some statistical way. This refers to the study of the influence of form parameters on the flow characteristics of the ship form. From the study a general trend of the influence of basic ship form parameters on the viscous resistance and its friction and pressure components could be evaluated. Also the relation between the form parameters and the separation area could be investigated.

The theory applied gives results which based on our previous knowledge can be accepted qualitatively. The calculations performed provide also many quantitative informations and reveal some new trends that should be confirmed experimentally on bodies of revolution and actual ship forms.

Received by the Editor, October 1982.

References

[1] J. Zazurca, *Calculation of Viscous Resistance of a Ship Form from that of Equivalent Bodies of Revolution* (in Spanish). Ingenieria Naval, No 44. 1976.

[2] Truong Sy Kap. *Calculation of the Potential Flow and Boundary Layer Characteristics of the Ship Form Based on Body of Revolution Analogy.* Ship Research Institute, Technical University of Gdańsk, Rep. No 911/MR-162/78.

[3] J. F.C. Conn, A. M. Ferguson, *Results obtained with a Series of Geometrically Similar Models.* Trans., The Royal Institute of Naval Architects, 1967.

[4] P. S. Granville, *Partial Form Factors from Equivalent Bodies of Revolution for Froude Method of Predicting Ship Resistance.* SNAME Paper No 9 presented at „Star Alpha", The First Ship Technology and Research Symposium, Washington, 26—29 Aug., 1975.

[5] W. Morgan, Proceedings of 14-th International Towing Tank Conference, 1976.

[6] G. Dyne, *A Theoretical Scale Effect Study on the Propulsion Coefficient of a Body of Revolution.* Symp. „Hydrodynamics of Ships and Offshore Propulsion Systems", Hovik Outside Oslo, 20—25 March, 1977.

[7] P. N. Joubert, T. J. Sinclair, P. H. Hoffman, *A Further Study of Bodies of Revolution.* Journal of Ship Research, 1976.

[8] G. E. Gadd, *Scale effect on stern separation and resistance of full hull form.* Naval Architect, R.I.N.A., No 6, 1977.

[9] L. Landweber, *Discussion of skin friction resistance and the effect of surface roughness*, by F. H. Todd. Trans. SNAME, 1951.

[10] G. Hughes, R. S. Cutland, *Viscous and wave components of ship model resistance.* Department of Trade and Industry, 1978.

[11] Series 60 — The effect of variation in ship proportion. Trans. SNAME.

[12] E. Freimanis, H. Lindgren, *Systematic tests with ship models with $C_B = 0.60$–0.75.* Rep. No 44, Goteborg, 1959.

[13] Ship Research Institute, Technical University of Gdańsk, Rep. No 109a/71.

[14] P. U. Chang, *Separation of Flow.* Pergamon Press, 1970, p. 182.

[15] Truong Sy Kap, *Influence of form parameters on ship viscous resistance components and flow separation.* Ship Research Institute, Technical University of Gdańsk, Rep. No 991/MR-203/78.

[16] L. G. Loitsansky, *Mechanics of Fluids and Gases* (in Russian). Moscow 1970.

Appendix 1

The principles of the calculation method

a. Velocity potential of the body of revolution

Calculation of the velocity potential as performed following Zazurca's work [1]. Fig. 6 shows the cylindrical system of coordinates adopted and the basic quantities involved. The body of revolution in the coordinate system is defined by

$$R = R_0(x).$$

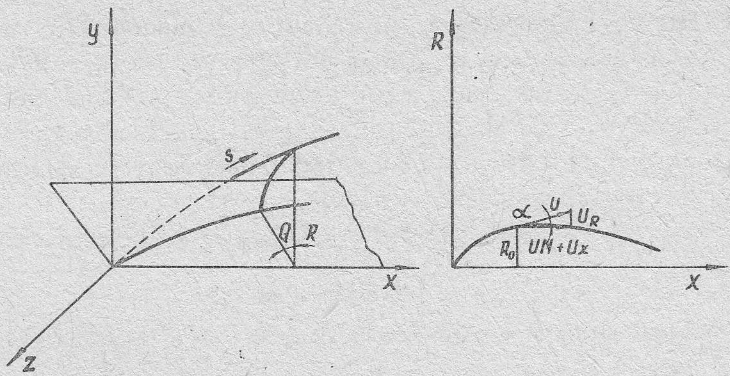

Fig. 6. Cylindrical system of coordinates adopted in calculation of flow characteristics

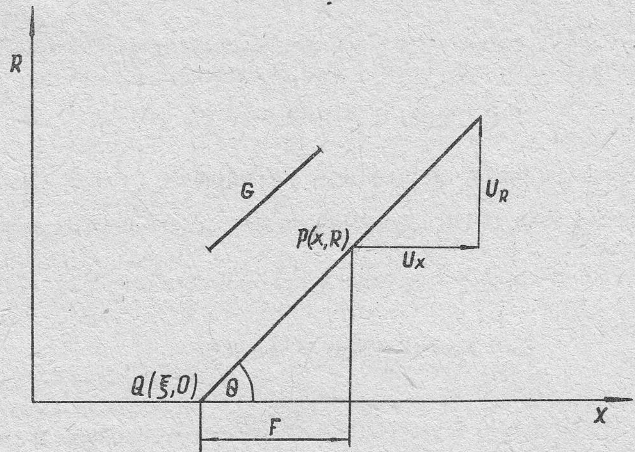

Fig. 7. Location of singularity and velocity components

Its motion can be described by the following velocity components

$$U_R \text{ — radial velocity,} \quad U \text{ — } UN+U_x \text{ — axial velocity.}$$

The resultant velocity potential of the flow is a sum of the potential of velocity in infinity U_x and the potential of the induced velocity $\varphi(x, R)$

$$\Phi = U_x + \varphi(x, R)$$

and it satisfies the Laplace's equation

$$\nabla^2 \Phi = 0.$$

The following boundary conditions are considered

1. If x or R approaches infinity, $U_x = U_R = 0$.
2. The resultant velocity vector must be tangent to the surface of the body at the point $R = R_0(x)$.

Fulfillment of condition 2 leads to the following expression for the velocity potential of the body

$$2UN \cdot S(x) = \int_0^L q(\xi) \frac{x-\xi}{(x-\xi)^2 + R_0^2} d\xi, \qquad (14)$$

where $S(x) = \pi R_0^2(x)$; $q(\xi)$ — strength of the singularity located at the point $Q(\xi, 0)$, Fig. 7.

The resultant velocity can be expressed as

$$U = \sqrt{(UN+U_x)^2+U_R}.$$

For $R = R_0$

$$U = U_e = \sqrt{[UN+(U_x)_{R=R_0}]^2+(U_R)^2_{R=R_0}}.$$

Since

$$(U_R)_{R=R_0} = R_0'[UN+(U_x)_{R=R_0}]$$

we have

$$U_e = \sqrt{1+R_0'}\,[UN+(U_x)_{R=R_0}].$$

The final equation for calculating the resultant velocity along the body of revolution is as follows

$$U_e = \sqrt{1+R_0^2}\left(UN+\frac{1}{4\pi}\int_0^L q(\xi)\frac{x-\xi}{[(x-\xi)^2+R_0^2]^{3/2}}d\xi\right). \tag{15}$$

Values of $q(\xi)$ can be found from an approximate solution of equation (14). The equation is a Fredholm equation of the first kind and can be substituted by a set of algebraic linear equations of the type

$$\sum_{m=1}^{n} A_K\cdot K(X_i, X_K)g(X_K) = f(X_i), \tag{16}$$

where $g(X_K)$ is the unknown function. A_K are coefficients found from the Tchebycheff formula $A_K = \frac{b+a}{n}$, X_K — are abscissae corresponding to the Tchebycheff division, X_i are abscissae corresponding to the section considered.

The set of equations (16) can be solved by means of the Gauss method [2].

b. Equivalent body of revolution

The friction resistance of the ship can be assumed to be equal to the friction resistance of the equivalent body of revolution. The equivalent body of revolution is defined by two conditions: the pressure field and the wetted surface. The pressure field of the ship form is obtained from that of the body of revolution for which the distribution along the length of the transverse section radius is obtained from the following relation

$$R = \sqrt{\frac{2S(x)}{\pi}}, \tag{17}$$

where $S(x)$ is a transverse section area of the ship form at distance x.

The radius of the equivalent body of revolution R_p adopted for calculation of the boundary layer characteristics is found from the formula

$$R_p = \frac{P}{\pi}, \tag{18}$$

where P is the wetted perimeter of the ship form section.

Appendix 2

Calculation of the boundary layer characteristics

To calculate the boundary layer characteristics the following equation for turbulent flow is adopted

$$\frac{d\theta}{dx}+(2+H)\frac{\theta}{U_e}\frac{dU_e}{d_x}+\frac{\theta}{R_0}\frac{dR_0}{dx} = \frac{1}{2}C_f'. \tag{19}$$

The above equation is solved by the so called parametric method, similar to that applied in the case of laminar flow. For the turbulent boundary layer the following parameters can be used

$$f = \frac{U_e'\theta}{U_e} G(R_n^{**}), \quad \xi = \frac{\tau}{\varrho U_e^2} G(R_n^{**}).$$

It can be shown that

$$\xi = \xi(f) \quad \text{and} \quad H = H(f).$$

With these parameters equation (19) can be transformed into the form

$$\frac{df}{dx} = \frac{U_e'}{U_e} F(f) + \frac{U_e''}{U_e'} - 2\frac{R_0'}{R_0} f, \tag{20}$$

where

$$F(f) = (1+m)\xi - [3+m+(1+m)H]f. \tag{21}$$

The function $G(R_n^{**})$ can be evaluated by different methods for the regions far away from the boundary layer separation point and close to that point. Loitsansky [16] suggested the following functions along the body for a completely turbulent boundary layer

$$G(R_n^{**}) = 153.2\ R_n^{**1/6}.$$

Thus for $m = \frac{1}{6}$

$$F(f) = \frac{7}{6} - \left(\frac{19}{6} + \frac{7}{6}H\right) f$$

can be obtained from eq. (21).

The function can be presented in the form

$$F(f) = a - bf,$$

where $a = 1.17$ and $b = 4.7 \div 4.8$.

Solution of eq. (20) leads to the following equation

$$f(x) = 1.17 \frac{U_e(x)}{U_e^{4.7} R_0^{7/6}} \int_0^x U(\xi)^{3.7} R(\xi)^{7/6} d\xi. \tag{22}$$

By means of the function $f(x)$ the following quantities can be found: the momentum thickness θ, tangential stress coefficient ξ, shape factor $H(f)$, local stresses τ_0 and skin friction resistance R_F

$$\theta = \frac{fU_e}{U_e' G(R_n^{**})}, \tag{23}$$

$$\xi = 1.0 + 0.1367f + 0.015f^2 + 0.00333f^3, \tag{24}$$

$$H = 1.4 - 0.070f + 0.02913f^2 + 0.01083f^3 + 0.001606f^4, \tag{25}$$

$$\tau_0 = \frac{\xi U_e^2 \varrho}{G(R_n^{**})}, \tag{26}$$

$$R_F = \int_S \tau_0 dS, \tag{27}$$

$$C_F = \frac{2R_F}{\varrho (UN)^2 S}. \tag{28}$$

In case of a body of large fullness the procedure for calculating the boundary layer characteristics will be the same as outlined above for the region some distance apart from the separation point, but it will differ for the region close to that point. In the latter case, after the function $f(x)$ has been found, the new function

$\bar{f}(x)$ should be introduced

$$\bar{f}(x) = \frac{f(x)}{f_s}, \tag{29}$$

where f_s is the shape factor at the point of separation estimated experimentally, $f_s = 3.3 \div 6.8$ [16].

For calculation of θ, ξ, H and τ_0 equations (23), (24), (25) and (26) are applied, respectively, with $\bar{f}(x)$ being used instead of the function f. The separation point is defined by the equality $\tau_0 = 0$.

Appendix 3

Numerical example of calculation of the ship viscous resistance components

The calculation method described in Appendices 1 and 2 was applied to compute the velocity potential, velocity distribution, boundary layer characteristics and viscous resistance components of a tanker model of the following characteristic parametes:

length on waterline	$L_{WL} =$ 8.549 m
length between perpendiculars	$L_{PP} =$ 8.374 m
mean draugth	$T =$ 0.568 m
breadth	$B =$ 1.373 m
displacement	$D =$ 5.525 kG
wetted surface	$S =$ 18.503 m^2
block coefficient	$C_B =$ 0.834

The calculated characteristics of an equivalent body of revolution, viz.

$$S(i) = \int_0^T Y(i)\,dT, \tag{30}$$

$$R(i) = \sqrt{\frac{2S(i)}{\pi}}, \tag{31}$$

$$R_P(i) = \frac{P}{\pi} \tag{32}$$

are presented in Fig. 8.

The potential $q(\xi)$ and the velocity along the hull were evaluated following equations (14) and (15). The boundary layer characteristics $\theta(i)$, $H(i)$ and τ_0 were calculated by means of equations (23), (25) and (26), respectively. The results of calculation for $V = 1.26$ m/s are shown in Fig. 9.

The skin friction resistance R_F and its coefficient C_F were calculated according to equations (27) and (28), respectively.

For the ship form considered in the present example the total resistance coefficient C_T is known from experiment for wide range of Froude numbers F_n. Assuming that in the non-wave-making range of F_n the only component of the total resistance is the viscous resistance,

$$C_T = C_V$$

and $C_V = C_F + C_P$ according to the assumption made previously.

Having the skin friction coefficient C_F calculated theoretically by the method described in Appendices 1 and 2 we have

$$C_P = C_V - C_F.$$

The form factors k_1 and k_2 are calculated using relations (6) and (9).

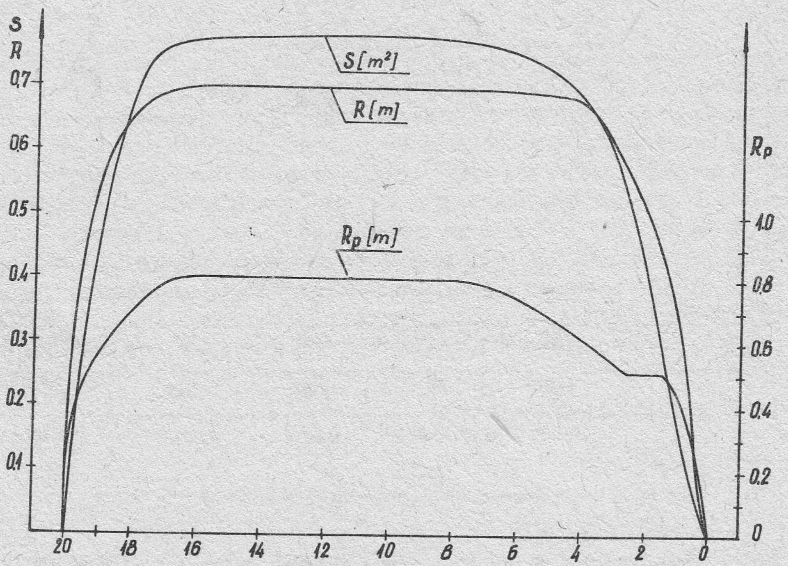

Fig. 8. Characteristics of equivalent body of revolution for the tanker

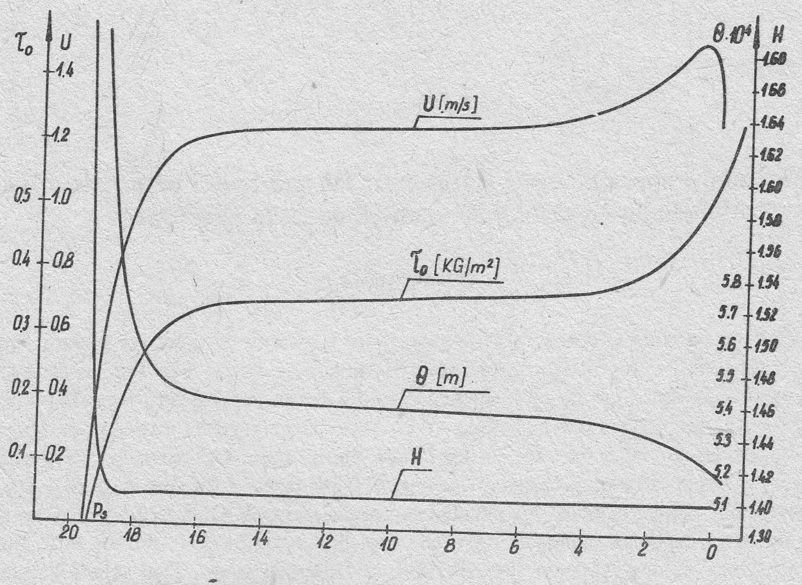

Fig. 9. Boundary layer characteristics of the tanker for the speed $V = 1.26$ m/s

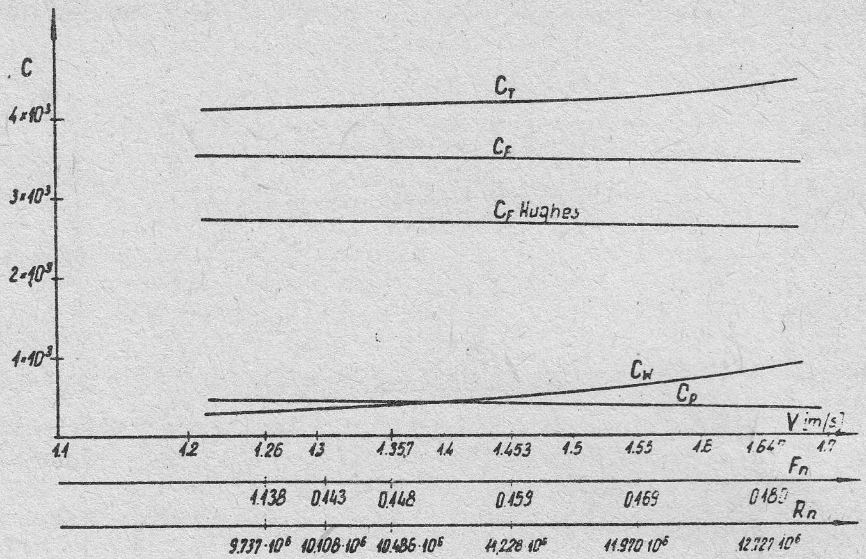

Fig. 10. Resistance components of the tanker calculated by the proposed method

As was stated above the point on the body surface at which $\tau_0 = 0$ was taken as the boundary layer separation point. The distance between the point and the trailing edge is designated by X_s and expressed nondimensionally as

$$X_s = \frac{X_s}{L} \cdot 100. \tag{33}$$

Fig. 10 presents the results of calculation for the given example.

Badanie składników oporu lepkości statku oraz ich zależności od parametrów kształtu kadłuba na podstawie analogii do ciała obrotowego

Streszczenie

Celem pracy jest badanie zależności składników oporu statku od parametrów kształtu kadłuba. Dla wyodrębnienia składników oporu, tzn. opór tarcia i ciśnienia, z oporu lepkości opracowano metodę obliczania oporu tarcia opierając się na koncepcji równoważnego ciała obrotowego. Zgodnie z tą koncepcją charakterystyki przepływu potencjalnego statku oraz charakterystyki warstwy przyściennej można obliczyć posługując się analogią kształtu statku i ciała obrotowego. Obliczony na tej podstawie opór tarcia zgadza się z wynikami badań eksperymentalnych. Opór tarcia policzono następnie dla 86 modeli statków, których opór całkowity znany był z badań eksperymentalnych. Obliczony opór tarcia przyrównany następnie do oporu lepkości znanego z doświadczenia dla „bezfalowego" obszaru liczb Froude'a pozwolił na wyznaczenie oporu ciśnienia spowodowanego lepkością wody. Oba składniki oporu: tarcia i ciśnienia wyznaczone dla rozważanych modeli są następnie przedmiotem analizy statystycznej, mającej na celu wyznaczenie ich zależności od parametrów kształtu kadłuba.

Исследование компонентов сопротивления вязкости судна а также их зависимости от параметров формы судна на основе аналогии к осесимметричному телу

Резюме

Целью работы является исследование зависимости компонентов сопротивления судна от параметров формы корпуса. Для выделения компонентов сопротивления, т.е. сопротивления трения и давления из сопротивления вязкости, разработан метод расчета сопротивления трения на основе идеи эквивалентного осесимметричного тела. Согласно с этой идеей характеристика потенциального течения судна, а также характеристики пограничного слоя можно вычислить пользуясь аналогиеи формы судна и осесимметричного тела. Вычисленное на этой основе сопротивление трения совпадает с результатами экспериментальных исследований. Вычисленное сопротивление трения, сравниваемое затем с сопротивлением вязкости, известным из опыта для „безволновой" зоны чисел Фруда, позволило определить сопротивление давления, вызванное вязкостью воды. Оба компоненты сопротивления: трения и давления, определенные для рассматриваемых моделей, являются затем предметом статистического анализа, целью которого является определение их зависимости от параметров формы корпуса.